



IMPROVED DROUGHT EARLY WARNING AND FORECASTING TO STRENGTHEN
PREPAREDNESS AND ADAPTATION TO DROUGHTS IN AFRICA
DEWFORA

A 7th Framework Programme Collaborative Research Project

**Meteorological drought forecasting (monthly to seasonal
forecasting) at regional and continental scale
ECMWF and CCAM meteorological data description**

**WP4-D4.1
August 2011**



Coordinator: Deltares, The Netherlands
Project website: www.dewfora.net
FP7 Call ENV-2010-1.3.3.1
Contract no. 265454





Page intentionally left blank



DOCUMENT INFORMATION

Title	Meteorological drought forecasting (monthly to seasonal forecasting) at regional and continental scale
Lead Author	ECMWF
Contributors	ECMWF, CSIR
Distribution	PU: Public
Reference	WP4-D4.1

DOCUMENT HISTORY

Date	Revision	Prepared by	Organisation	Approved by	Notes
01/06/2011	V0				Draft version v1
26/07/2011	V1				Draft version v2
16/08/2011	V2				Final version

ACKNOWLEDGEMENT

The research leading to these results has received funding from the European Union's Seventh Framework Programme (FP7/2007-2013) under grant agreement N°265454



Page intentionally left blank



SUMMARY

This report is a contribution of the work package WP4 of DEWFORA project. WP4 is responsible the drought forecasting at different temporal and geographical scales. Part of the work includes the preparation and extraction of datasets for implementation of the different drought indicators. The meteorological data includes: (i) the European Centre for Medium/Range Weather Forecasts (ECMWF) ERA-Interim reanalysis and long-range weather forecasts, and (ii) the Council for Scientific and Industrial Research (CSIR) in South Africa conformal-cubic atmospheric model (CCAM) seasonal forecasting system. An application example of the meteorological data in deriving drought indicators is presented.



Page intentionally left blank



TABLE OF CONTENTS

- 1. INTRODUCTION..... 1**
- 2. ECMWF DATA..... 3**
 - 2.1 INTRODUCTION 3
 - 2.2 ERA-INTERIM..... 3
 - 2.3 ENSEMBLE FORECASTS 5
 - 2.3.1 Monthly forecasts..... 6
 - 2.3.2 Seasonal forecasts 8
 - 2.4 DATA DELIVERED TO PARTNERS 10
- 3. CCAM DATA..... 11**
 - 3.1 INTRODUCTION 11
 - 3.2 DATA AND METHOD FOR SST PREDICTION 11
 - 3.3 SST FORECAST RESULTS..... 12
 - 3.4 WAY FORWARD 14
- 4. DROUGHT INDICATORS..... 15**
- 5. REFERENCES..... 19**



LIST OF FIGURES

Figure 1. Top: Mean annual precipitation in ERA-Interim (left) and in GPCP (right). Bottom: Mean annual cycle of precipitation over Africa ($40^{\circ}\text{S} < \text{latitude} < 35^{\circ}\text{N}$, $20^{\circ}\text{W} < \text{longitude} < 45^{\circ}\text{E}$) from ERA-Interim (black) and GPCP (red). The vertical lines represent the interannual variability of the mean over Africa in the form of \pm one standard deviation.	5
Figure 2. Mean seasonal differences between ERA-Interim and GPCP for Winter (top left), Spring (top right), Summer (bottom left) and Autumn (bottom right).	5
Figure 3. Scores of the Monthly forecast system (green symbols) of the 500 hPa geopotential height for the Northern hemisphere as function of lead time, compared against a forecasts based on the climatology (blue symbols) and persistence (red symbols). The top panel displays the Root Mean Square Errors (RMSE). The bottom panel displays the anomaly correlation. The plots are based on all the real-time monthly forecasts since 7 October 2004, when the monthly forecasting system became operational.	8
Figure 4. Niño3.4 SST anomaly plume ($^{\circ}\text{C}$) (red) of the ECMWF system 3 forecast from 1 November 2009 compared with observations (black).	9
Figure 5. Anomaly correlation coefficient of near-surface temperature for the ECMWF seasonal forecast system. Hindcasts period 1981-2005 with start in June for months 2 to 4 (August October). Black dots for values significantly different from zero with 95% confidence.	10
Figure 6. January Niño3.4 SST anomaly ($^{\circ}\text{C}$) single- and multi-model forecasts over the 28-year retrospective forecast period. The mean squared error (MSE) skill score and Spearman rank correlations (and associated p-values) are included for each lead-time.	12
Figure 7. January Niño3.4 SST forecast skill for all lead times, for each single model and for the multi-model (MM).	13
Figure 8. Spearman rank correlations and p-values for January SST forecasts at a 2-month lead time.	13
Figure 9. The January 1998 SST anomaly ($^{\circ}\text{C}$) forecast made at a 2-month lead-time.	14
Figure 10. Grid-point temporal correlation of SPI-12 derived from ERAI and GPCP monthly precipitation.	16
Figure 11. Fraction of the central East Africa ($25^{\circ}\text{E} < \text{Longitude} < 40^{\circ}\text{E}$, $15^{\circ}\text{S} < \text{Latitude} < 0^{\circ}\text{N}$) in drought derived from the SPI-12 using ERAI (red) and GPCP(blue). The solid lines represent the fraction of the region where SPI12 is below -1, and the shading areas the uncertainty by accounting for thresholds between -0.6 and -1.4.	16
Figure 12. SPI12 for June 2011 using ERAI precipitation.	17



LIST OF TABLES

Table 1. Overview of ECMWF products	3
Table 2. Drought indexes, needed data for their calculation and availability in forecasts and reanalysis.	15



Page intentionally left blank



1. INTRODUCTION

This report is a contribution of the work package WP4 of DEWFORA project. WP4 is responsible for the drought forecasting at different temporal and geographical scales. The report is integrated in task 4.1. The meteorological data includes: (i) the European Centre for Medium/Range Weather Forecasts (ECMWF) ERA-Interim reanalysis and long-range climate forecasts, and (ii) the Council for Scientific and Industrial Research (CSIR) in South Africa conormal-cubic atmospheric model (CCAM) seasonal forecasting system.

The meteorological models outputs are described in the next two sections in terms of their configurations (e.g. resolution) and available data. This data is available to all the partners in the project for use in task 4.2 and 4.3 and in the case studies in WP6. Section 4 presents an application example of the meteorological data in deriving drought indicators.



2. ECMWF DATA

2.1 INTRODUCTION

A full set of available data from ECMWF with some information on configuration is provided in Table 1. The following sections provide a brief description of the European ECMWF ERA-Interim reanalysis and long-range climate forecasts.

Table 1. Overview of ECMWF products

Atmosphere global forecasts
<ul style="list-style-type: none"> Forecast to ten days from 00 and 12 UTC at 16 km resolution and 91 levels (in 2011/12: ~137 levels).
Ocean wave forecasts
<ul style="list-style-type: none"> Global forecast to ten days from 00 and 12 UTC at 28 km resolution. European waters forecast to five days from 00 and 12 UTC at 11 km resolution.
51-member ensemble prediction system
<ul style="list-style-type: none"> To day 15 from 00 and 12 UTC (to day 32 on Thursdays at 00 UTC, in 2011: also on Mondays + 46d on the 15th of each month); 32 km resolution up to day 10, then 65 km, and 62 vertical levels (in 2011: ~95 levels); 12 UTC with persisted SST up to day 15, 00 UTC with persisted SST up to day 10 and then coupled ocean model (in 2011 coupled both at 00 and 12 UTC); Coupled ocean has horizontally varying resolution ($\frac{1}{3}$ to 1°), 29 vertical levels (in 2011 new ocean model NEMO and NEMOVAR DA); Coupled wave mode.
Seasonal forecasts: Atmosphere-ocean coupled model
<ul style="list-style-type: none"> 41-member global forecasts to seven months (in 2011: System 4); atmosphere: 120 km resolution, 62 levels (80km, 91 levels); ocean: horizontally-varying resolution ($\frac{1}{3}^\circ$ to 1°), 29 levels (NEMO and NEMOVAR); re-forecast suite: 11 members x 25 years (15 members x 30 years, 1981-2005)
Reanalysis
<ul style="list-style-type: none"> Since January 1979 to present (near real time update); Atmosphere: 80 km horizontal resolution with 62 vertical levels; 6 hourly analysis, 12 hour 4D-Var assimilation; 10 days forecasts (at 00 and 12 UTC).

2.2 ERA-INTERIM

ERA-Interim (hereafter ERAI) is the latest global atmospheric reanalysis produced by ECMWF. ERAI covers the period from 1 January 1979 onwards, and continues to be extended forward in near-real time. Gridded data products include a large variety of 3-hourly surface parameters, describing weather as well as ocean-wave and land-surface conditions, and 6-hourly upper-air parameters covering the troposphere and stratosphere. Vertical



integrals of atmospheric fluxes, various synoptic and daily monthly averages, and other derived fields have also been produced. Berrisford et al. (2009) provide a detailed description of the ERAI product archive. Information about the current status of ERAI production, availability of data online, and near-real time updates of various climate indicators derived from ERAI data, can be found on the internet¹. Dee et al. (2011) presents a detailed description of the ERAI model and data assimilation system, the observations used, and various performance aspects.

The dynamical core of the atmospheric model is based on a spectral representation for the basic dynamical variables, a hybrid vertical coordinate, and a semi-Lagrangian semi-implicit time stepping scheme. The ERAI configuration has a spectral T255 horizontal resolution (compared to T159 for ERA-40), which corresponds to approximately 79 km spacing on a reduced Gaussian grid (125 km for ERA-40). The vertical resolution is unchanged, using 60 model levels with the top of the atmosphere located at 0.1 hPa. The land surface scheme used is TESSEL², the predecessor of HTESSEL (Balsamo et al. 2009). The ERAI reanalysis is produced with a sequential data assimilation scheme, advancing forward in time using 12-hourly analysis cycles. In each cycle, available observations are combined with prior information from a forecast model to estimate the evolving state of the global atmosphere and its underlying surface. This involves computing a variational analysis of the basic upper-air atmospheric fields (temperature, wind, humidity, ozone, surface pressure), followed by separate analyses of near-surface parameters (2m-temperature and 2m-humidity), soil moisture and soil temperature, snow, and ocean waves. The analyses are then used to initialise a short-range model forecast, which provides the prior state estimates needed for the next analysis cycle. The data assimilation thus produces a coherent record of the global atmospheric evolution for the entire period of reanalysis, which is consistent with available observations. The ERAI archive contains 6-hourly gridded estimates of 3-dimensional meteorological variables, and 3-hourly estimates of a large number of surface parameters and other 2-dimensional variables. Figure 1 and Figure 2 compare the total and seasonal precipitation over Africa between ERA-Interim and the Global Precipitation Climatology Project (GPCP) version 2.1 (Huffman et al. 2009).

¹ <http://www.ecmwf.int/research/era>

² <http://www.ecmwf.int/research/ifsdocs/CY28r1/Physics/Physics-08-02.html>

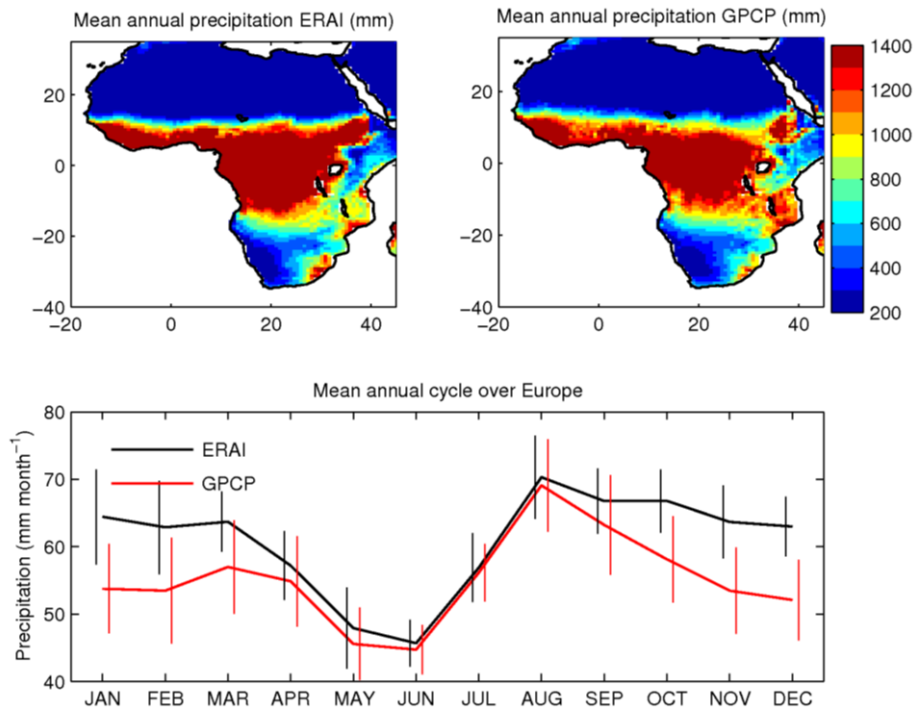


Figure 1. Top: Mean annual precipitation in ERA-Interim (left) and in GPCP (right). Bottom: Mean annual cycle of precipitation over Africa ($40^{\circ}\text{S} < \text{latitude} < 35^{\circ}\text{N}$, $20^{\circ}\text{W} < \text{longitude} < 45^{\circ}\text{E}$) from ERA-Interim (black) and GPCP (red). The vertical lines represent the interannual variability of the mean over Africa in the form of \pm one standard deviation.

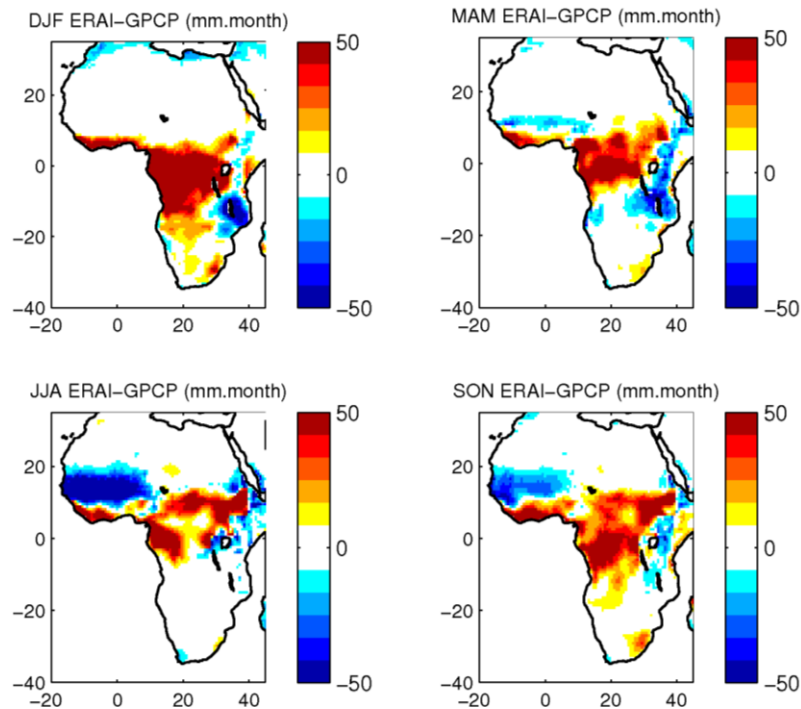


Figure 2. Mean seasonal differences between ERA-Interim and GPCP for Winter (top left), Spring (top right), Summer (bottom left) and Autumn (bottom right).

2.3 ENSEMBLE FORECASTS

Two ensemble forecasting systems are currently operational at ECMWF: VarEPS (variable resolution ensemble prediction system) for medium-range weather forecasting and seasonal



forecasting. VarEPS produces weather forecasts out to 32 days, whereas seasonal forecasting produces forecasts out to 7 months.

Medium-range and monthly weather forecasting is essentially an atmospheric initial value problem. Since the time scale is too short for variations in the ocean significantly to affect the atmospheric circulation, the ECMWF medium-range weather forecasting system is based on atmospheric-only integrations. SSTs are simply persisted.

Seasonal forecasting, on the other hand, is justified by the long predictability of the oceanic circulation (of the order of several months) and by the fact that the variability in tropical SSTs has a significant global impact on the atmospheric circulation. Since the oceanic circulation is a major source of predictability in the seasonal scale, the ECMWF seasonal forecasting system is based on coupled ocean-atmosphere integrations. Seasonal forecasting is also an initial value problem, but with much of the information contained in the initial state of the ocean.

It what follows the description will concentrate on the monthly and seasonal forecasts as these are the only types of forecasts specifically requested so far. Partners are encouraged to also request the medium range predictions.

2.3.1 Monthly forecasts

The main goal of monthly forecasting is to fill the gap between the medium-range (up to day 15) and the seasonal (up to 7 months) systems and produce forecasts for the time range 10 to 30 days. The time range 10 to 30 days is probably still short enough that the atmosphere retains some memory of its initial state and it may be long enough that the ocean variability has an impact on the atmospheric circulation. Therefore, the monthly forecasting system has been built as a continuation of the medium-range VARePS, but in ocean-atmospheric coupled mode after day 10.

The coupled model consists of the ECMWF atmospheric model (the same cycle as the deterministic forecast), coupled to an ocean general circulation model which is a version of the Hamburg Ocean Primitive Equation model (HOPE), developed at the Max Plank Institute for Meteorology, Hamburg. The ocean model has lower resolution in the extratropics but higher resolution in the equatorial region, in order to resolve ocean baroclinic waves and processes which are tightly trapped at the equator. The ocean model has 29 levels in the vertical. The atmosphere and ocean communicate with each other through a coupling interface, called OASIS, developed at CERFACS, France. The atmospheric fluxes of momentum, heat and fresh water are passed to the ocean every hour and, in exchange, the ocean sea surface temperature (SST) is passed to the atmosphere.

The real-time VarEPS/monthly forecasting system is a 51-member ensemble of 32-day integrations. The first 10 days are performed at TL639L62 (0.28x0.28 degrees) resolution forced by persisted SST anomalies (updated every 24 hours). After day 10, the model is



coupled to the ocean model and has a resolution of TL319L62 (0.56x0.56 degrees). The extension of VarEPS to 32 days is performed every Thursday.

After 10 days of coupled integrations, the model drift begins to be significant. It displays similar patterns to seasonal forecasting after 6 months of integrations, but with less amplitude. The strategy for dealing with model drift is straightforward. The ocean, atmosphere and land surface are initialized to be as close to reality as possible, and calculate the forward evolution of the system as best it can using numerical approximations of the laws of physics. No "artificial" terms are introduced to try to reduce the drift of the model and no steps are taken to remove or reduce any imbalances in the coupled model initial state. The effect of the drift on the model calculations is estimated from previous integrations of the model in previous years (referred as hindcasts or climatology). The drift is removed from the model solution during the post-processing. An additional motivation for creating a model climatology is that after about 10 days of forecasts, the spread of the ensemble is very large. Therefore, the probability distribution function (pdf) of the model climatology needs to be evaluated, in order to detect any significant difference between the ensemble distribution of the real-time forecast and climatology.

In the present system, the climatology is a 5-member ensemble of 32-day VarEPS/monthly integrations, starting on the same day and month as the real time forecast for each of the past 18 years. For instance, the first starting date of the real-time forecast was 27 March 2002. The corresponding climatology is a 5-member ensemble starting on 27 March 1990, 27 March 1991, ..., 27 March 2001. The 5-member ensemble is thus integrated with 18 different starting dates. This represents a total of 90 integrations and constitutes the 90-member ensemble of the climatology. Figure 3 displays an example of the verification of the monthly forecast. The scores are the anomaly correlation and root mean square error of the 500 hPa geopotential height over the Northern Hemisphere. The anomaly correlation is computed as the spatial correlation between the forecast anomaly and the verifying analysis anomaly. The Root Mean Square Errors are the geographical average of the squared differences between the forecast and the analysis valid for the same time. The scores are computed from the forecasts and compared against a forecast based on the climatology and on persistence.

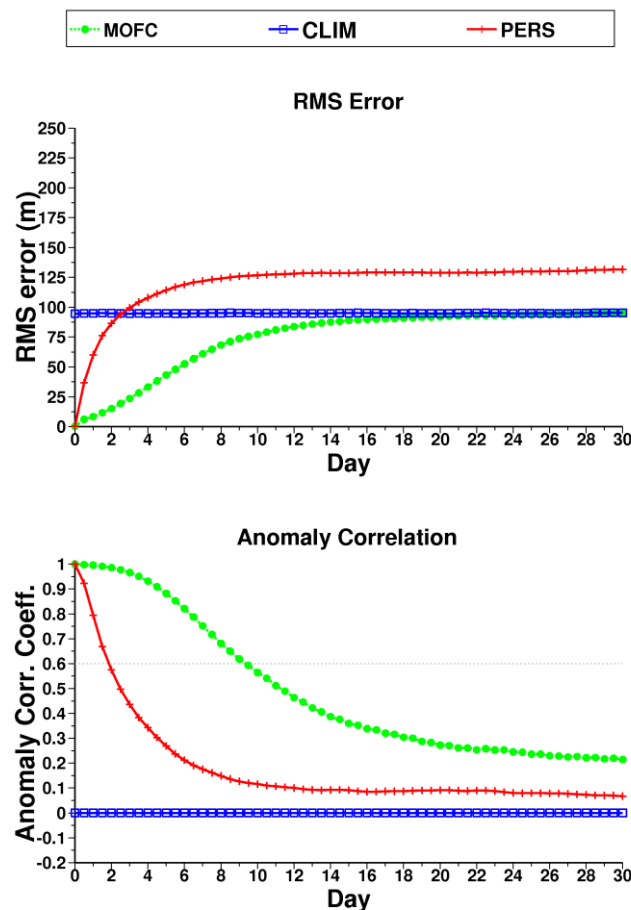


Figure 3. Scores of the Monthly forecast system (green symbols) of the 500 hPa geopotential height for the Northern hemisphere as function of lead time, compared against a forecasts based on the climatology (blue symbols) and persistence (red symbols). The top panel displays the Root Mean Square Errors (RMSE). The bottom panel displays the anomaly correlation. The plots are based on all the real-time monthly forecasts since 7 October 2004, when the monthly forecasting system became operational.

2.3.2 Seasonal forecasts

Seasonal forecasting is the attempt to provide useful information about the "climate" that can be expected in the coming months. The seasonal forecast is not a weather forecast: weather can be considered as a snapshot of continually changing atmospheric conditions, whereas climate is better considered as the statistical summary of the weather events occurring in a given season. The principal aim of seasonal forecasting is to predict the range of values which is most likely to occur during the next season. In some parts of the world, and in some circumstances, it may be possible to give a relatively narrow range within which weather values are expected to occur. Such a forecast can easily be understood and acted upon; some of the forecasts associated with strong El Niño events fall into this category. More typically, the probable ranges of the weather differ only slightly from year to year. Forecasts of these modest shifts might be useful for some but not all users.

The atmospheric component of the coupled model is the ECMWF IFS (Integrated Forecast System) model version 31r1. This model version was introduced for medium-range forecasting on 12th September 2006. The horizontal resolution used for seasonal forecasts is

TL159 (1.125x1.125 degrees). The ocean model and coupling strategy between the atmosphere and ocean follows the same procedure as the monthly forecasts (see previous section).

The seasonal forecasts consist of a 41 member ensemble. The ensemble is constructed by combining the 5-member ensemble ocean analysis with SST perturbations and the activation of stochastic physics. The forecasts run for 7 months. Any coupled model that runs in seasonal forecast mode suffers from bias (as in the monthly forecasts) - the climate of the model forecasts differs to a greater or lesser extent from the observed climate. Since seasonal forecast signals are often small, this bias needs to be taken into account, and must be estimated from a previous set of forecasts. Also, it is vital that users know the skill of a seasonal forecasting system if they are to make good use of it in real applications, and again this requires a set of forecasts from earlier dates. A set of re-forecasts (otherwise known as hindcasts or back integrations or just referred as climatology) are thus made starting on the 1st of every month for the years 1981-2005. They are identical to the real-time forecasts in every way, except that the ensemble size is only 11 rather than 41. The data from these forecasts is available to users of the real-time forecast data, to allow them to calibrate their own real-time forecast products using their own techniques. An example of the forecast is presented in Figure 4 for the Niño3.4 anomaly from November 2009. The forecast system was able predict the time evolution of the strong positive sea surface temperature anomaly and its decay in the following months. Figure 5 represents the anomaly correlation of near surface temperature of the seasonal forecast system during the hindcast period (1981-2005) for the forecasts started in June and valid for month 2 to 4 (August to October). This is an example of verification of the seasonal forecast system performed at ECMWF.

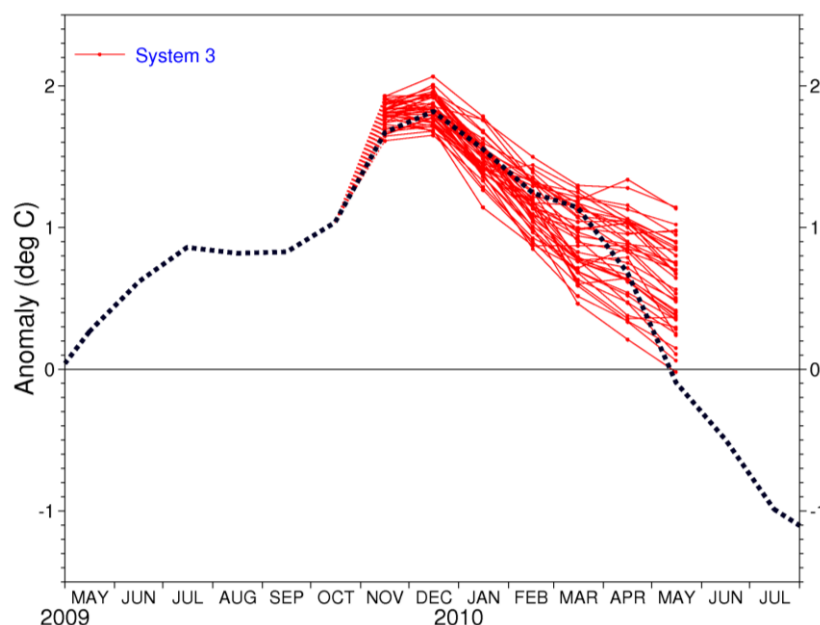


Figure 4. Niño3.4 SST anomaly plume (°C) (red) of the ECMWF system 3 forecast from 1 November 2009 compared with observations (black).

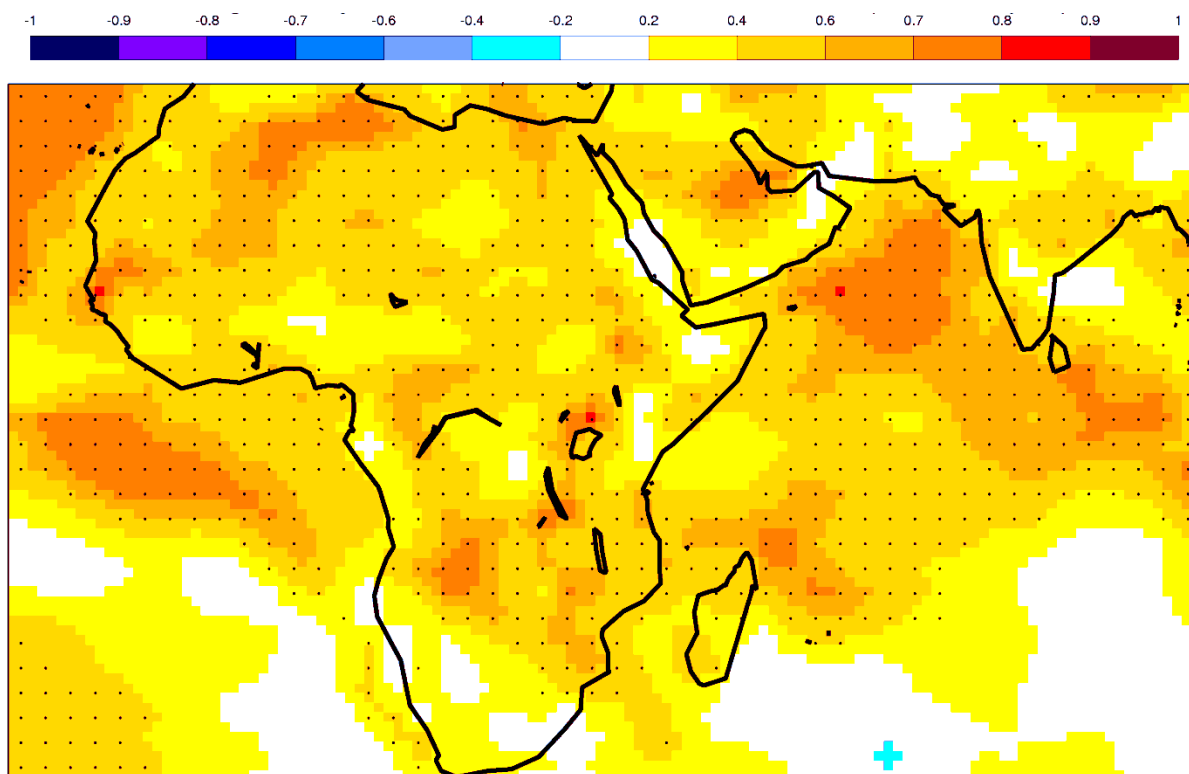


Figure 5. Anomaly correlation coefficient of near-surface temperature for the ECMWF seasonal forecast system. Hindcasts period 1981-2005 with start in June for months 2 to 4 (August October). Black dots for values significantly different from zero with 95% confidence.

2.4 DATA DELIVERED TO PARTNERS

We encourage partners to use the ECMWF data finder¹ to specify requests (without using the order function). Data are usually delivered in the GRIB format². ECMWF provides tools such as the GRIB API³ to read, write and manipulate that data format under an Apache Licence.

¹ <http://www.ecmwf.int/products/data/archive/finder.html>

² <http://www.wmo.ch/pages/prog/www/DPS/FM92-GRIB2-11-2003.pdf>

³ http://www.ecmwf.int/products/data/software/grib_api.html



3. CCAM DATA

3.1 INTRODUCTION

The conformal-cubic atmospheric model (CCAM) as seasonal forecasting system is currently being run operationally at the Council for Scientific and Industrial Research (CSIR) in South Africa. The forecasts are provided to the South African Weather Service (SAWS) as input into their multi-model forecasting system. An example of such a multi-model forecast can be found in the web¹.

The CCAM is currently being forced with persisted sea-surface temperature (SST) anomalies in order to produce the forecasts assimilated into the multi-model system of SAWS. The CCAM system was developed prior to the start of DEWFORA project and can therefore in its current form not be considered as a new development. However, the CCAM is currently being configured to generate a 28-year set of hindcasts to be produced as a result of forcing the CCAM with predicted, as opposed to persisted, SST anomalies. A description of how the 28-year SST forecast set was generated follows.

3.2 DATA AND METHOD FOR SST PREDICTION

The archived sub-surface temperature forecast data of two CGCMs are considered here, and they are respectively the ECHAM4.5-MOM3-DC2 (12 ensemble members; 74.25°S to 65.25°N) and the ECHAM4.5-GML-CFSSST (12 ensemble members; 46°S to 46°N). Each of these coupled model forecast sets is available from January 1982 to present. The model data are obtained from the data library of the International Research Institute for Climate and Society. The observed SST data sets used are the 1°x1° resolution data of NOAA's OI.v2, and the 2°x2° resolution data of NOAA's NCDL ERSST version3b.

The SST forecast system presented here is based on a multi-model approach by including forecasts from a statistical model (canonical correlation analysis – CCA) that uses the most recent 3-month mean antecedent global ERSST field as predictor and the OI.v2 global SST as predictand, and from the two CGCMs. The three models are employed to produce a 28-year set of retro-active SST forecasts from 1982/83 to 2009/10 for lead-times up to 6 months. The CCA option of the Climate Predictability Tool (CPT) is used for the statistical model forecasts, and also to project the subsurface temperature data of the CGCMs onto the 1°x1° resolution OI.v2 grid. This procedure of downscaling or recalibrating the coarse resolution CGCM forecasts to the OI.v2 grid is advantageous since all the forecasts are subsequently produced on a common high-resolution grid and the forecast skill of the models is further enhanced. The ensemble means of the coupled models are used in the CPT and the forecasts are created using a cross-validation design with a large 7-year-out window, and by considering a maximum of 9 EOF predictor and 9 EOF predictand modes. The final step in

¹ http://rava.qsens.net/themes/climate_template/seasonal-forecasts/PCP_SEA_S-AFRICA.gif/view

the retro-active forecast process is to average the three global forecasts in order to produce an equal weights set of multi-model forecasts. The same procedure is followed to produce forecasts operationally every month. The operational forecasts and verification statistics are presented on the website of the South African Risk and Vulnerability Atlas (<http://rava.qsens.net/>).

For the statistical model (CCA) and the ECHAM4.5-GML-CFSSST system (GML), forecasts are produced near the beginning of the month, and for the ECHAM4.5-MOM3-DC2 system (MOM) currently near the end of the month. The convention used here to describe the lead-times is as follows. A 1-month lead-time for the former two model systems implies that there are about three weeks from the issuance of the forecast to the beginning of the forecast month. For example, a 1-month lead-time forecast for the month of December is produced at the beginning of November. For the ECHAM4.5-MOM3-DC2 system, there are at least four weeks between the production of the forecast and the forecast target month. For example, December forecasts at a 1-month lead-time are produced near the end of October.

3.3 SST FORECAST RESULTS

The January retro-active forecast performance for the Niño3.4 area (5°N to 5°S; 170° to 120° W) is shown in Figure 6. These forecasts are highly skilful during austral summer, with the lowest skill found during winter.

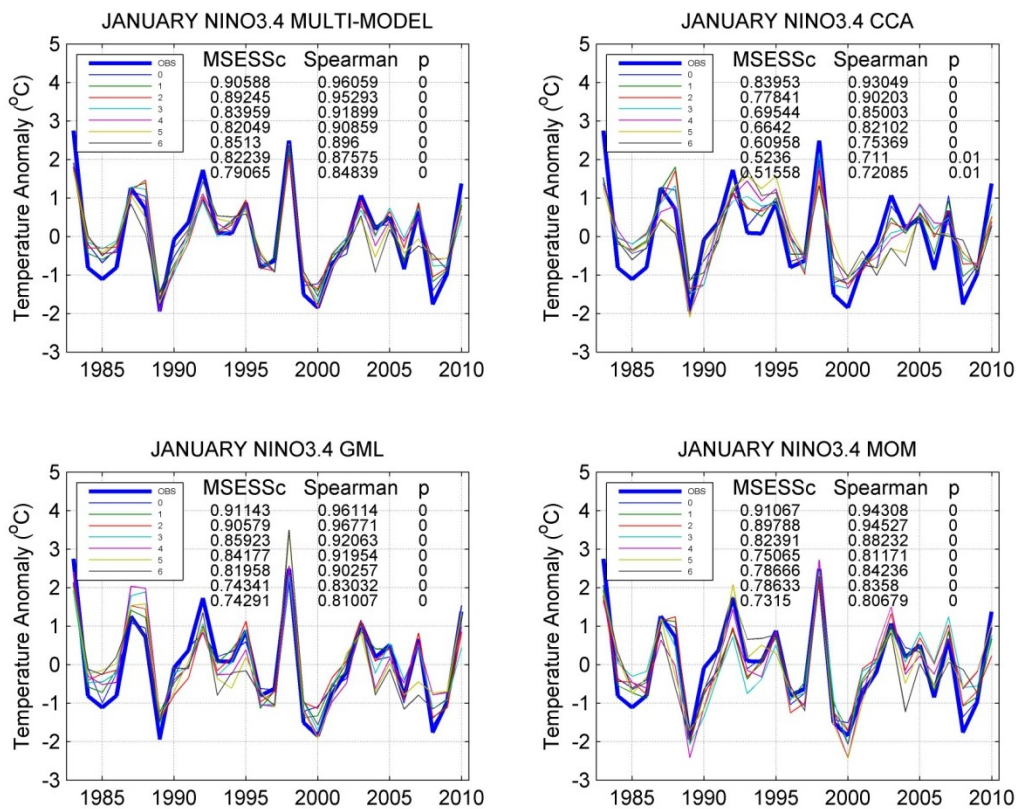


Figure 6. January Niño3.4 SST anomaly (°C) single- and multi-model forecasts over the 28-year retro-active forecast period. The mean squared error (MSE) skill score and Spearman rank correlations (and associated p-values) are included for each lead-time.

Niño3.4 SST forecast skill levels of the individual models and of the multi-model do not differ significantly, but the lowest skill is found for the statistical model. Moreover, the multi-model does not outscore the individual models throughout as is demonstrated in Figure 7. Here the multi-model only starts to outscore the January Niño3.4 SST forecast of the best single model at lead-times exceeding 3 months.

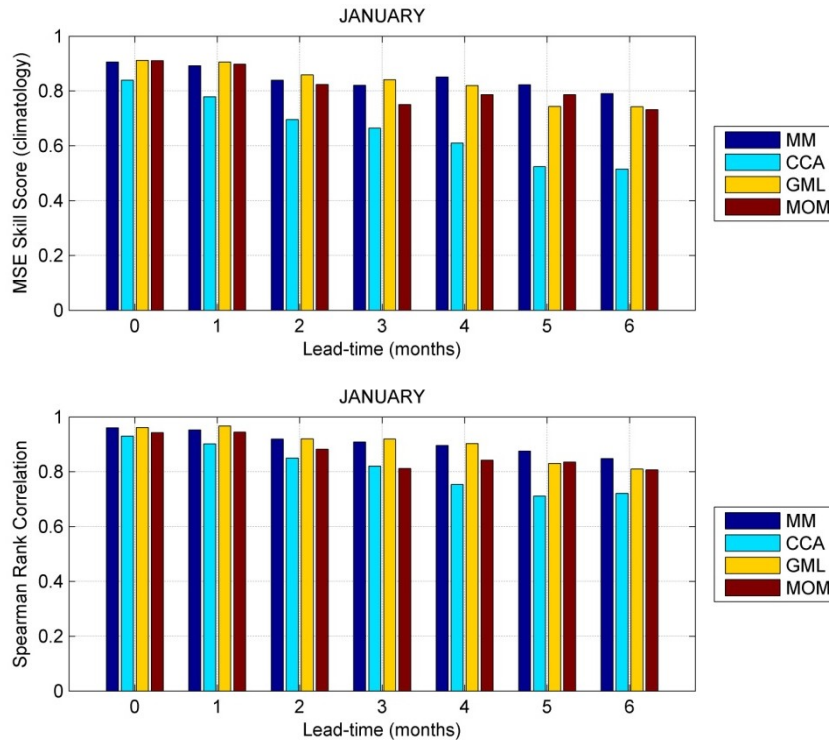


Figure 7. January Niño3.4 SST forecast skill for all lead times, for each single model and for the multi-model (MM).

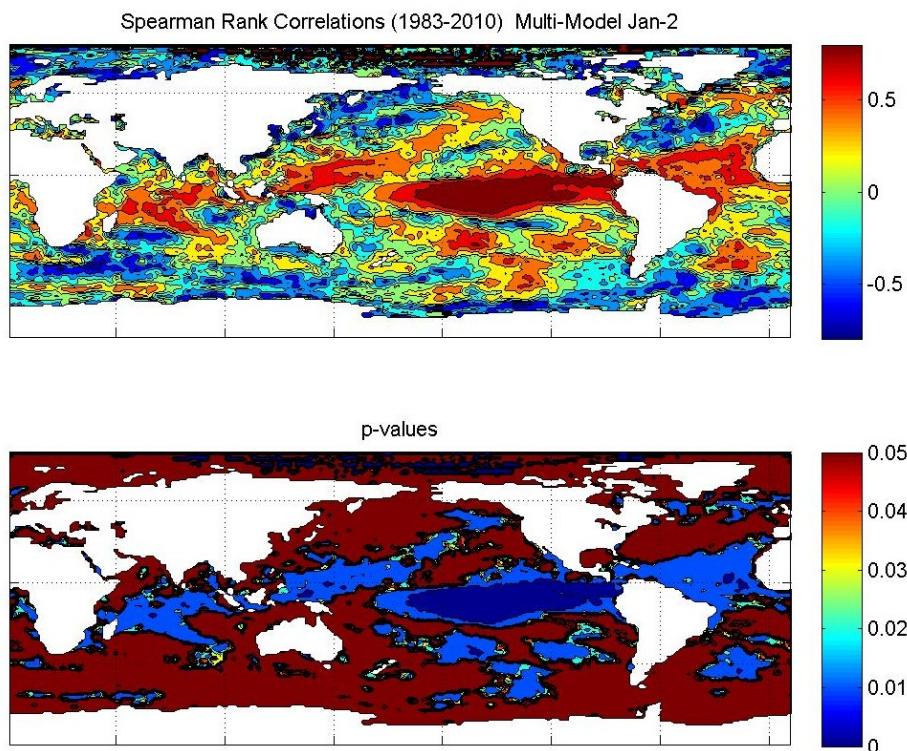


Figure 8. Spearman rank correlations and p-values for January SST forecasts at a 2-month lead time.

Figure 8 shows the Spearman rank correlation values and associated p-values for January global SST forecasts at a 2-month lead-time. Take note that high skill values are mainly restricted to the tropics, especially over the equatorial Pacific Ocean. Finally, Figure 9 shows a typical forecast: The January global SST anomaly forecasts during the strong 1997/98 El Niño event.

The full sets of retro-active and verification statistics, and operational SST forecast fields are available on request (full annual cycle, for lead-times from 0 to 6 months). The forecasts are already being used by a number of institutions running AGCMs operationally. For example the University of Cape Town¹, and the South African Weather Service².

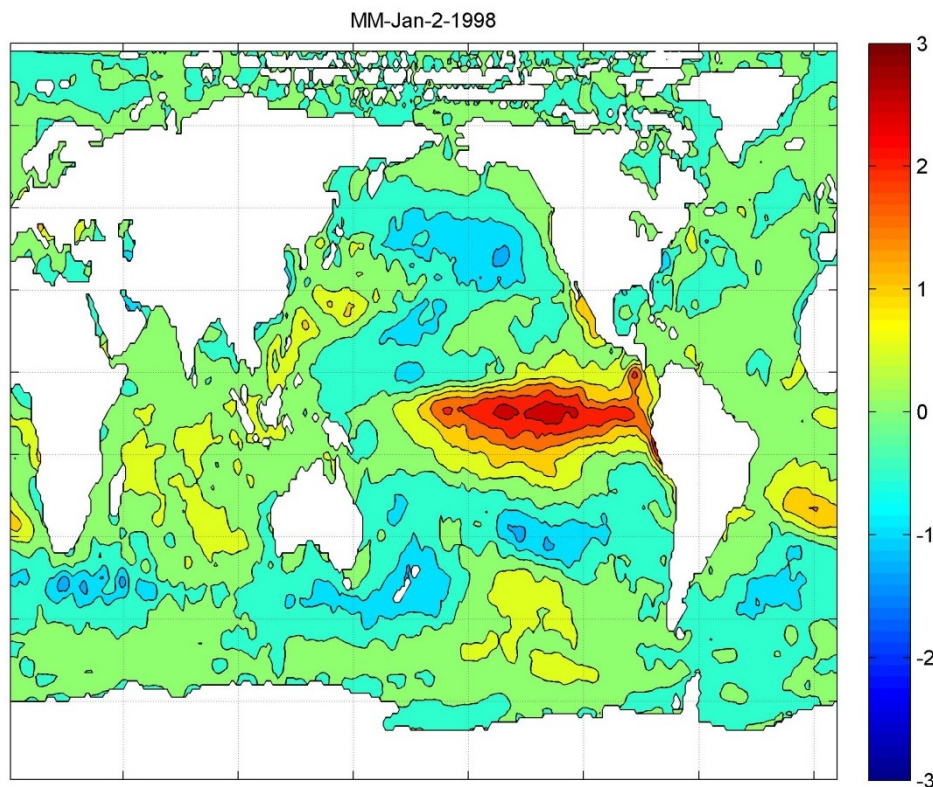


Figure 9. The January 1998 SST anomaly (°C) forecast made at a 2-month lead-time

3.4 WAY FORWARD

CCAM 28-year hindcast runs forced with the above described multi-model global SST anomalies will commence in August, 2011. The first target season will be the austral mid-summer period of December to February. An ensemble of 10 members for each forecast lead-time is to be generated.

¹ <http://www.gfcsa.net/CSAG/fcstSSTs/>

² <http://old.weathersa.co.za/LONGTERM/lrf.html>

4. DROUGHT INDICATORS

Table 2 presents an overview of drought indexes that can be evaluated using the meteorological data. Table 2 does not intend to provide a full review of drought related indices, such can be found in the literature (e.g. Heim 2002). It serves as a list of possible indicators that could be used to validate the medium- to long-range meteorological forecasts that are available to the partners. The deliverable 4.5 provides a review of available global land surface and hydrological models that can use these meteorological forecasts for drought forecasting in Africa at different temporal and spatial scales.

Table 2. Drought indexes, needed data for their calculation and availability in forecasts and reanalysis.

Indicator	Needed data	Availability in forecast
Standardized precipitation index [SPI; (Mckee et al. 1993)]	Monthly precipitation	Available in all products
Standardized Precipitation Evapotranspiration index [SPEI; (Vicente-Serrano et al. 2010)]	Monthly precipitation Monthly potential evaporation (can be derived from temperature)	Precipitation is all products. Potential evaporation can be derived from temperature also available in all products.
Standardized runoff index (SRI;(Shukla and Wood 2008)	Monthly runoff	Available in all products
Soil moisture (Sheffield et al. 2004) (Dutra et al. 2008)	Monthly soil moisture	Available in all products
Palmer Drought Severity Index [PDSI; (Palmer 1965)]	Precipitation, temperature	Available in all products

Indicators which are computed from model fields may need to be compared to the same indicator calculated from observations, when available to fully understand all non-linear interactions. Figure 10 displays the grid-point correlations of SPI at 12 months time-scale (SPI12) calculated using ERA-Interim and GPCP precipitation datasets. In the mid-latitudes there is a good agreement between the two indexes derived from different precipitation datasets. However, over the tropical regions, the low correlations show that on a yearly time scale the interannual variability of ERA-Interim is significantly different from GPCP. To further exemplify these differences, the fraction of area in drought in Central East Africa derived from ERA-Interim and GPCP is displayed in Figure 11. The major drought events identified

by GPCP in the 90's and 20's, are also captured by ERA-Interim but with a lower spatial extension. On the other hand, in the 80's, ERA-Interim shows larger drought extension than GPCP. This is an ongoing research topic, to identify and address the main problems of the reanalyses, that is strongly constrained by the lack of a dense network of long in-situ observations. Further results will be presented in the following project reports. GPCP is based in in-situ and remote sensing data, however it was discontinued in September 2009, limiting its application to near real time monitoring of drought conditions. Figure 12 is an example of this monitoring, displaying the SPI12 for June 2011. Just as an example, it is possible to identify the severe drought in the Horn of Africa, that is causing an humanitarian crisis in the region (OCHA 2011)

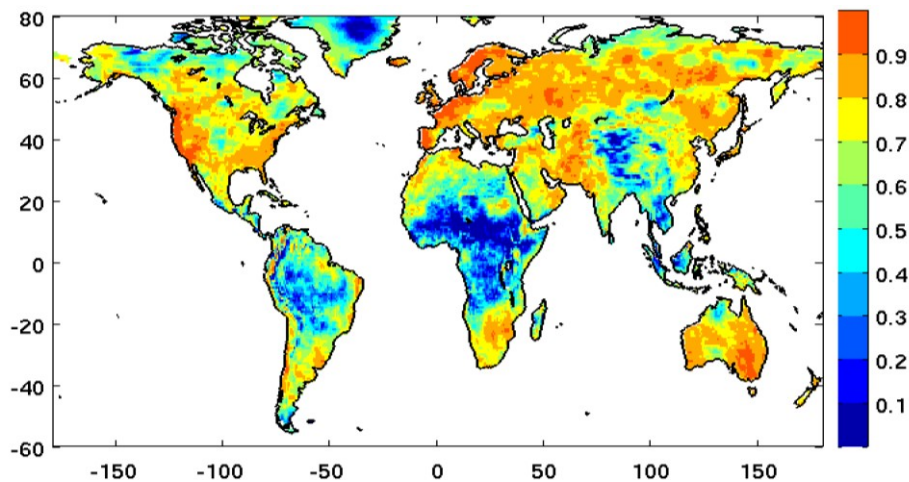


Figure 10. Grid-point temporal correlation of SPI-12 derived from ERAI and GPCP monthly precipitation.

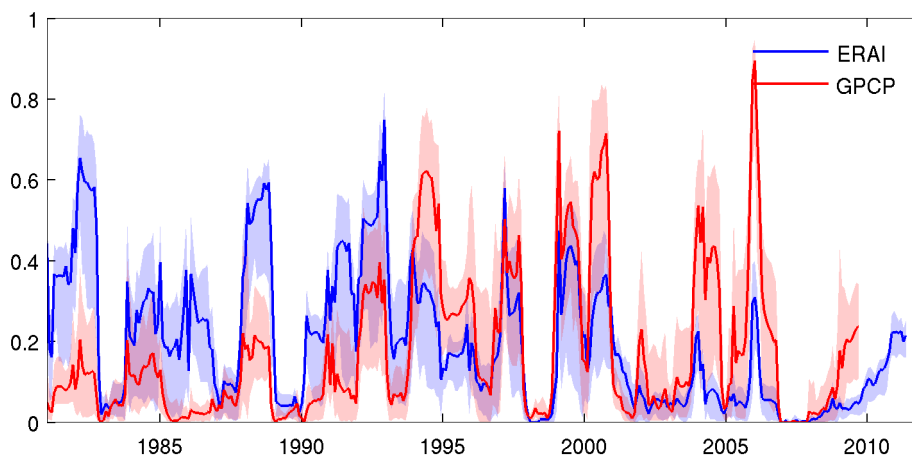


Figure 11. Fraction of the central East Africa ($25^{\circ}\text{E}<\text{Longitude}<40^{\circ}\text{E}$, $15^{\circ}\text{S}<\text{Latitude}<0^{\circ}\text{N}$) in drought derived from the SPI-12 using ERAI (red) and GPCP(blue). The solid lines represent the fraction of the region where SPI12 is below -1, and the shading areas the uncertainty by accounting for thresholds between -0.6 and -1.4.

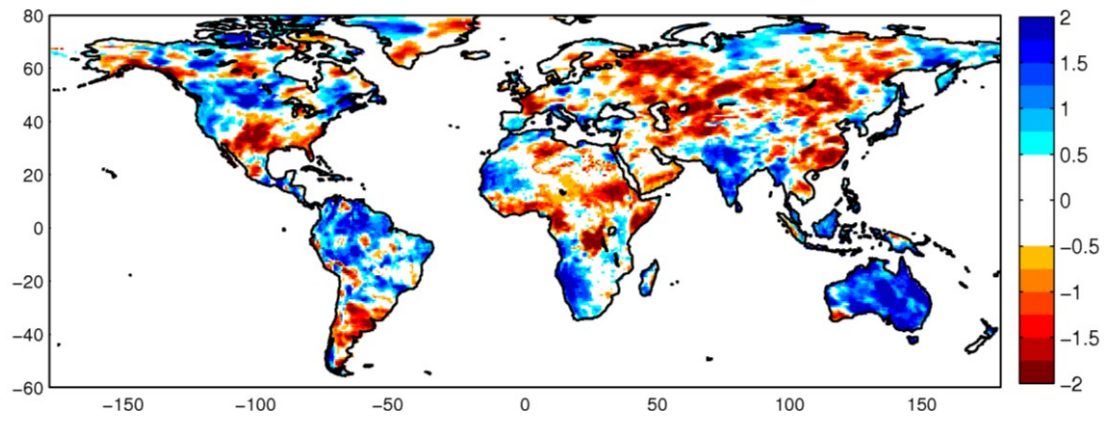


Figure 12. SPI12 for June 2011 using ERAI precipitation.



5. REFERENCES

- Balsamo, G., P. Viterbo, A. Beljaars, B. Van den Hurk, A. K. Betts, and K. Scipal, 2009: A revised hydrology for the ECMWF model: Verification from field site to terrestrial water storage and impact in the Integrated Forecast System, *J. Hydrometeor.*, **10**(3), 623-643 doi: 610.1175/2008JHM1068.1171.
- Berrisford, P., D. Dee, M. Fielding, M. Fuentes, P. Kallberg, S. Kobayashi, and S. M. Uppala, 2009: The ERA-Interim Archive, *ERA Report Series*, **No. 1**, ECMWF, Shinfield Park, Reading, UK.
- Dee, D. P., and Coauthors, 2011: The ERA-Interim reanalysis: configuration and performance of the data assimilation system, *Quart. J. Roy. Meteor. Soc.*, **137**(656), 553-597, doi: 10.1002/qj.828.
- Dutra, E., P. Viterbo, and P. M. A. Miranda, 2008: ERA-40 reanalysis hydrological applications in the characterization of regional drought, *Geophys. Res. Lett.*, **35**, L19402, doi:19410.11029/12008GL035381.
- Heim, R. R., 2002: A review of twentieth-century drought indices used in the United States, *Bull. Amer. Meteor. Soc.*, **83**(8), 1149-1165.
- Huffman, G. J., R. F. Adler, D. T. Bolvin, and G. Gu, 2009: Improving the global precipitation record: GPCP Version 2.1, *Geophys. Res. Lett.*, **36**(17), L17808, doi: 10.1029/2009gl040000.
- Mckee, T. B., N. J. Doesken, and J. Kleist, 1993: The relationship of drought frequency and duration to time scales. *Eight Conference on Applied Climatology*.
- OCHA (UN Office of the Coordination of Humanitarian Affairs), June 2011: Eastern Africa Drought Humanitarian Report No. 3
- Palmer, W. C., 1965: *Meteorological drought*. U.S. Dep. of Commerce, Res. Pap. 45, 58 pp.
- Sheffield, J., G. Goteti, F. H. Wen, and E. F. Wood, 2004: A simulated soil moisture based drought analysis for the United States, *J. Geophys. Res.*, **109**(D24), -.
- Shukla, S., and A. W. Wood, 2008: Use of a standardized runoff index for characterizing hydrologic drought, *Geophys. Res. Lett.*, **35**(2), L02405, doi: 10.1029/2007gl032487.
- Vicente-Serrano, S. M., S. Begueria, and J. I. Lopez-Moreno, 2010: A Multiscalar Drought Index Sensitive to Global Warming: The Standardized Precipitation Evapotranspiration Index, *J. Climate*, **23**(7), 1696-1718, doi: Doi 10.1175/2009jcli2909.1.